

Vertical motions in the Aegean volcanic arc: evidence for rapid subsidence preceding volcanic activity on Milos and Aegina

D.J.J. van Hinsbergen^{a,*}, E. Snel^b, S.A. Garstman^b, M. MăruŃeanu^c,
C.G. Langereis^{a,d}, M.J.R. Wortel^a, J.E. Meulenka^{a,b}

^aFaculty of Earth Sciences, Vening Meinesz Research School of Geodynamics (VMSG),
Utrecht University, Budapestlaan 4, 3584 CD Utrecht, The Netherlands

^bFaculty of Earth Sciences, Institute for Paleoenvironments and Paleoclimate Utrecht (IPPU),
Utrecht University, Budapestlaan 4, 3584 CD Utrecht, The Netherlands

^cGeological Institute of Romania, Str. Caransebes nr.1, RO-79678 Bucharest 32, Romania

^dPaleomagnetic Laboratory 'Fort Hoofddijk', Budapestlaan 17, 3584 CD Utrecht, The Netherlands

Received 3 November 2003; received in revised form 19 May 2004; accepted 11 June 2004

Abstract

Late-orogenic extension in the Aegean region has been ongoing since the late Eocene or early Oligocene. Contemporaneously, numerous volcanic centres developed. In the south-central Aegean region, Plio-Pleistocene volcanism formed a number of islands. On two of these—Milos and Aegina—a sequence of late Miocene and Pliocene marine sediments underlie the oldest volcanoclastics. To determine whether extension of the Aegean lithosphere played a role in the formation and location of the early Pliocene volcanoes of the Aegean, we aimed to reconstruct the vertical motion history as it occurred prior to the onset of volcanism. To this end we reconstructed the paleobathymetry evolution using foraminifera recovered from sedimentary sections in the lower Pliocene of Milos and Aegina. Age dating on the Milos sections was based on bio-magneto- and cyclostratigraphy; from Aegina only bio- and magnetostratigraphy were available. The results show that prior to the onset of volcanism on both islands, many hundreds of metres of early Pliocene subsidence occurred—on Milos even 900 m between 5.0 and 4.4 Ma. It is unlikely that extension of the Aegean lithosphere led to melting of the underlying mantle. However, the extension probably did play a significant role in the timing of the onset of Pliocene volcanic activity in the Aegean. The position of the volcanic centres is probably the result of the depth of the subducted slab below the Aegean and the formation of a network of extensional faults in the overriding Aegean lithosphere.

© 2004 Elsevier B.V. All rights reserved.

Keywords: volcanism; integrated stratigraphy; Milankovitch cyclicity; Greece; geohistory; paleobathymetry

1. Introduction and geological setting

After the main phase of late Mesozoic and Tertiary collision between the African and Eurasian plates,

lithospheric extension started to fragment the Aegean area in the course of the early Miocene (see [Gautier et al., 1999](#), for a review). During the lithospheric extension subduction has been ongoing, continuing a compressional regime in the external part of the Aegean domain. Behind and crosscutting the external outer Aegean, extensional basins formed, as well as volcanic

* Corresponding author. Fax: +31-30-253-2648.

E-mail address: hins@geo.uu.nl (D.J.J. van Hinsbergen).

centres (McKenzie, 1978a; Le Pichon and Angelier, 1979; Fytikas et al., 1984). Since the late Miocene, volcanic centres have developed in the southern part of the Aegean (Fig. 1), notably during the early Pliocene (4–2.5 Ma) and the middle Pleistocene to Holocene (1 Ma–recent; e.g. Fytikas et al., 1984).

In tectonically active settings, volcanism can generally be associated with melting due to subduction of hydrated lithosphere or extension of the lithosphere leading to partial melting as a result of extension-induced (adiabatic) decompression. In the Aegean example, where both subduction and extension occur

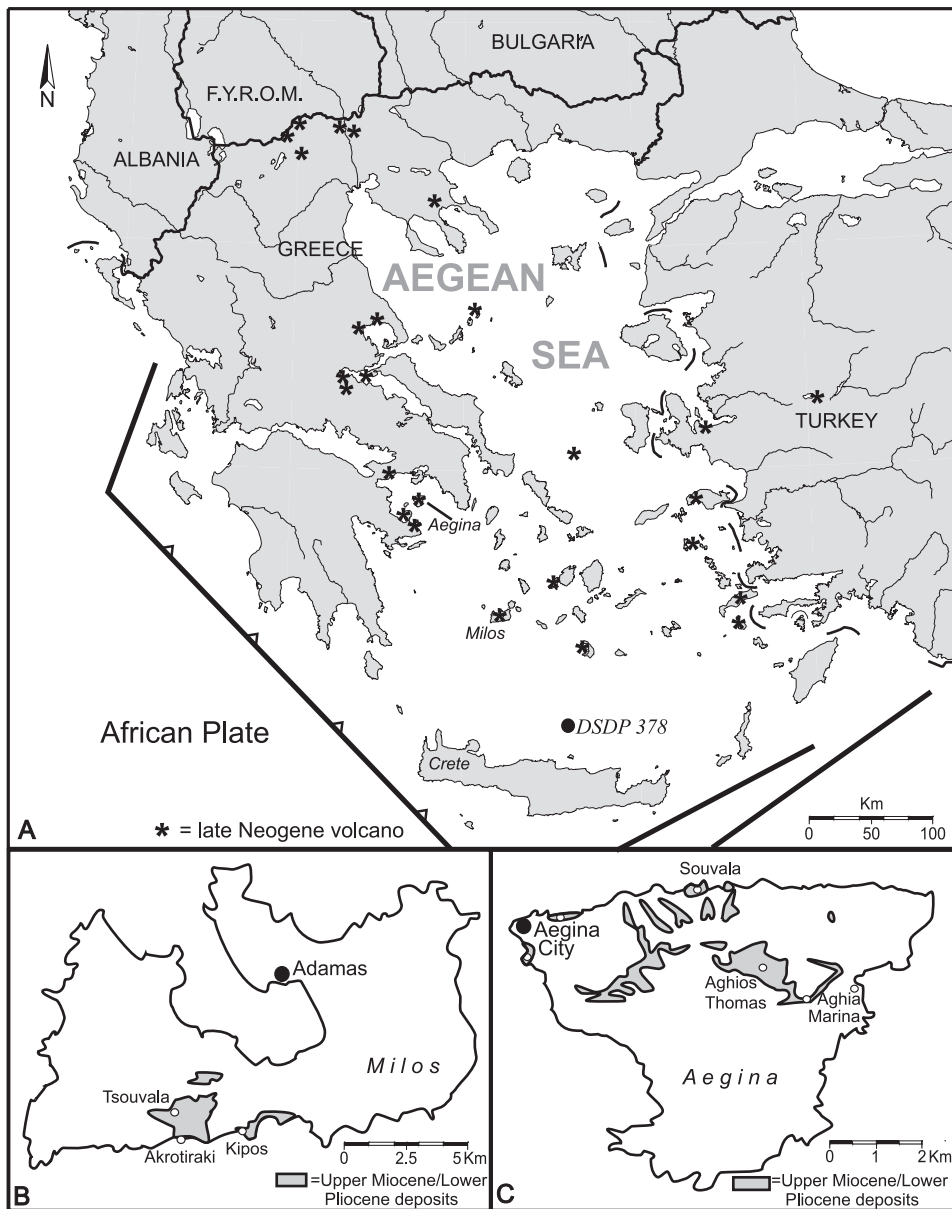


Fig. 1. (A) Map of Aegean area. Locations of Neogene volcanoes taken from Pe-Piper and Piper (2002); (B, C) maps with the selected sections on the islands of Milos and Aegina, respectively.

simultaneously, Pe and Piper (1972) and Briquieu et al. (1986) consider Aegean volcanism to be the result of melting associated with subduction of African lithosphere. Subduction has been ongoing since the late Mesozoic (Chapter 2). Thus, the question arises why volcanism was initiated in the southern Aegean in the early Pliocene, instead of being active throughout the entire subduction history. Pe-Piper and Hatzipanagiotou (1997) suggested that volcanism was triggered by a combination of extension of the overriding lithosphere and subduction and Perissoratis (1995) suggested that an early Pleistocene change in fault patterns led to the formation of the Santorini volcanic centre.

If rapid crustal extension played a significant role in the origin of Aegean volcanism, one would expect rapid pre-volcanic subsidence on the site of the present-day volcanoes. To test this, we aimed to carry out a vertical motion study on the basis of paleobathymetry fluctuations (following Steckler and Watts, 1978; Watts et al., 1982; Van Hinsbergen et al., submitted for publication) and a detailed integrated stratigraphic study to derive high-resolution timing of vertical motions preceding the onset of volcanism.

Promising successions were reported by Benda et al. (1979), Meulenkamp (1979) and Fytikas et al. (1986) from the upper Miocene–lower Pliocene of Milos and Aegina islands (Fig. 1), where volcanism developed in the course of the early Pliocene (Müller et al., 1979; Fytikas et al., 1986).

1.1. Milos

The oldest Neogene sediments unconformably overlie metamorphosed basement along the southern coast of Milos (Fig. 1; Fytikas, 1977; Meulenkamp, 1979). These Neogene sediments can be subdivided into Units A, B and a series of volcanoclastic sediments that unconformably overlie unit B (Figs. 2 and 3a).

Unit A contains 80 m of fluvio-lacustrine, brackish, and shallow marine conglomerates, sandstones, dolomites and occasional, reefal (coral) limestone. The top 20 m of Unit A contains a well-recognisable *Limnocardium* mould-bearing lacustrine limestone bed amidst intercalations of shallow marine hardgrounds, slumped marls and sand- and limestones (see also Meulenkamp, 1979).

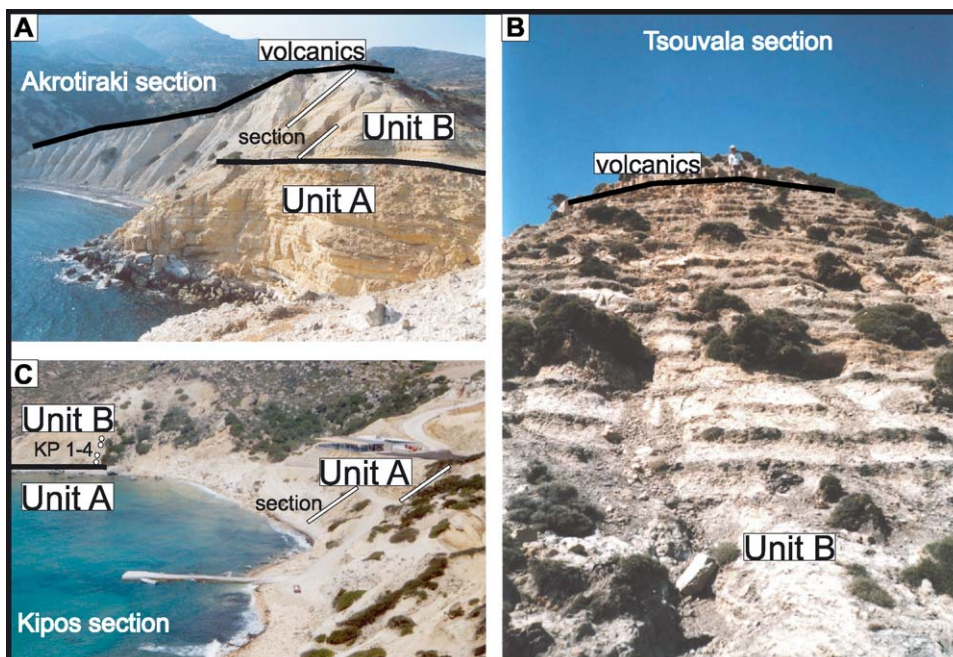


Fig. 2. Photograph of the sections on Milos. (A) Akrotiraki; (B) Tsouvala; (C) Kipos and position of samples KP 1–4.

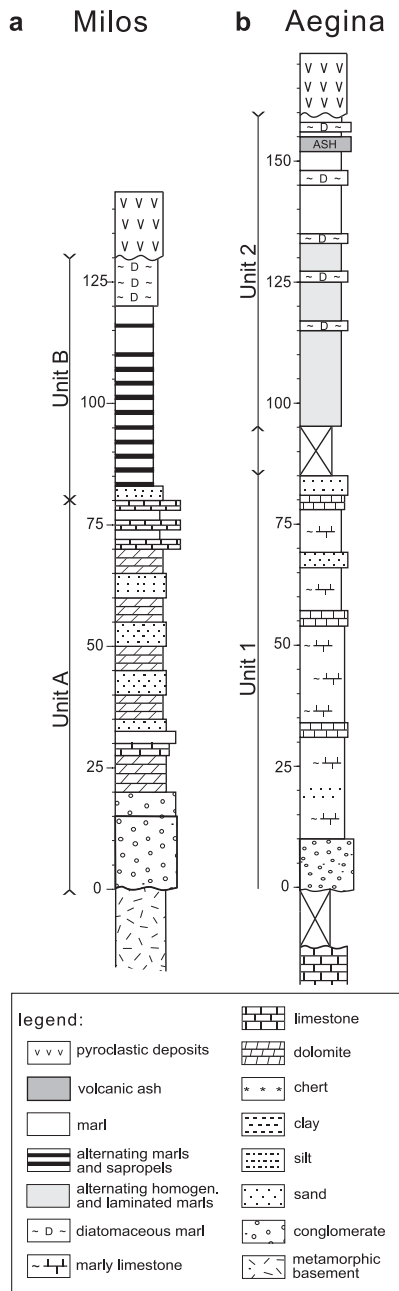


Fig. 3. Composite lithostratigraphic columns of the Neogene sediments on (a) Milos and (b) Aegina.

The overlying Unit B (Figs. 2 and 3a) was deposited in a marine environment. It locally starts with a 2-m-thick sandy base, containing pycnodonts and shark teeth, followed by a rhythmic alternation of marine

marls and sapropels. The top of the unit consists of diatomaceous (sandy) marls. The thickness of Unit B varies between 25 and 60 m because of the irregular character of an unconformity, which separates this unit from the overlying volcanoclastic series having ages of 3.5 ± 0.14 Ma and younger (Fig. 2; Fytikas et al., 1986).

A selection of three sections was made to construct a composite record covering a maximum time-interval. The section of Akrotiraki (Figs. 1, 2A and 4a) comprises the upper 18 m of Unit A (samples AT V–IX), the lower 30 m of Unit B (samples Gr 10.431–536) and 2 m of the overlying volcanics. The Tsouvala section (Figs. 1, 2B and 4b) contains 28 m of the marl–sapropel alternations of Unit B (samples Gr 10.151–245) and 2 m of the lowermost part of the overlying volcanics. Scarce outcrops of limestones of Unit A are present, but the transition to Unit B is not exposed. Both the upper part of Unit A and Unit B display mm-sized biotite-bearing volcanic ash intercalations (ashes 1–5 in Fig. 4). The third—Kipos—section (Figs. 1, 2C and 4c) is 21 m thick and consists of alternating shallow marine sands, marls and limestones (upper part of Unit A; samples Gr 10.541–586). A hundred metres further to the west, marly siltstones and sandstones of Unit B were sampled (KP 1–4; Fig. 2C), which directly overlie the uppermost hardground of Unit A. Severe fracturing made it impossible to correlate samples KP 1–4 to section Kipos, but the presence of the transition from Unit A to Unit B enabled correlation to section Akrotiraki (KP 2 in Fig. 4a). Section Kipos can be correlated with section Akrotiraki through the beds with *Limnocardium*-moulds exposed at the base of both sections. From the three sections on Milos, 99, 95 and 32 levels were sampled for paleomagnetic purposes from the Akrotiraki, Tsouvala and Kipos sections, respectively (Fig. 4).

1.2. Aegina

The Neogene sedimentary sequence of Aegina (Fig. 3b) unconformably overlies folded, unmetamorphosed Mesozoic carbonates, radiolarites and siliciclastics. The Neogene deposits crop out in the northern part of the island (Fig. 1). The central and southern parts of Aegina are covered by late Pliocene and Pleistocene volcanoclastics (Müller et al., 1979; Pe-Piper et al.,

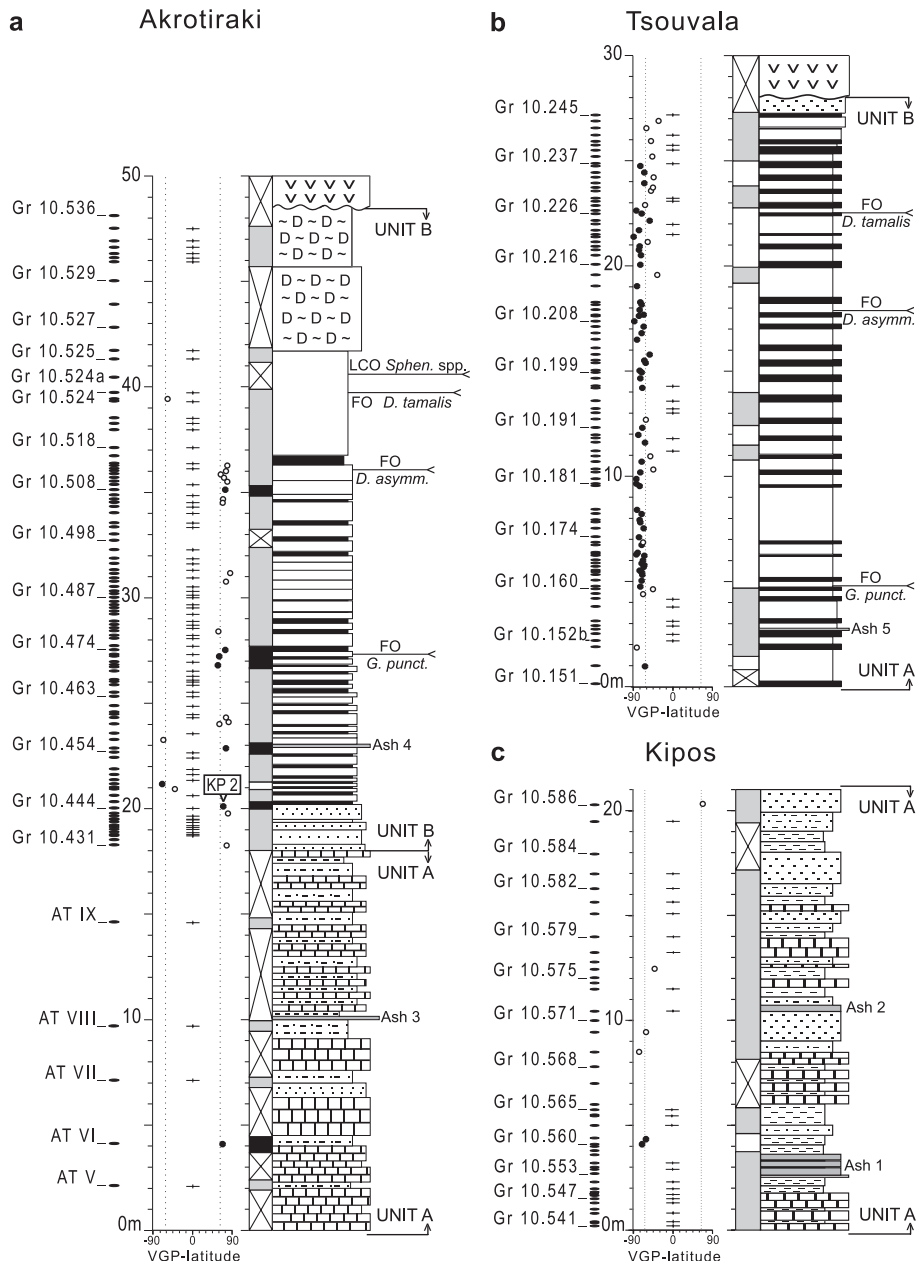


Fig. 4. Lithostratigraphic columns of the analysed sections on Milos, including the recorded bio-events. Gr (and other) numbers correspond to samples collected and held by the Faculty of Earth Sciences, Utrecht University. (a) Akrotiraki section. Sample KP 2 was taken from a laterally equivalent outcrop (Fig. 2B); (b) Tsouvála section; (c) Kipos section. Lithology, samples and paleomagnetic results, represented as virtual geomagnetic polar (VGP) latitude, with polarity Zone interpretation. Closed (open) circles denote projections of (less) reliable ChRM directions; '+' denotes inconclusive results (Fig. 6a). In the polarity column black (white) denotes normal (reversed) polarity; grey indicates less reliable and inconclusive polarity; white plus cross is used for intervals without data. *Sphen. spp.* = *Sphenolithus* spp.; *D. tamalis* = *Discoaster tamalis*; *D. asymm.* = *Discoaster asymmetricus*; *G. punct.* = *Globorotalia puncticulata*. For lithology keys: see Fig. 3.

1983; Morris, 2000). The oldest reported Neogene sediments (Unit 1) are continental conglomerates, grading upward into (at least) 75 m of marls, sands and marly limestones of lacustrine and brackish facies, containing brackish water molluscs and ostracods (Rögl et al., 1991). A sequence of at least 70 m of alternating laminated and homogeneous marls (Unit 2) overlies Unit 1 (Benda et al., 1979). The contact between the two Units is not exposed. Unit 2 contains a volcanic ash layer, and is unconformably overlain by an andesitic volcanoclastic series (Figs. 3 and 5; Pe, 1973; Müller et al., 1979; Pe-Piper et al., 1983).

Approximately 25 m of Unit 1 were studied by Rögl et al. (1991) in the Souvala section along the northern coast (Figs. 1 and 5a), while Unit 2 was described and sampled in the Aghios Thomas section (Benda et al., 1979) a few kilometers inland (Figs. 1 and 5b).

We resampled the Souvala section (Aeg 1–19 for paleomagnetic purposes and So 1–61 for biostratigraphic analysis) and logged an additional 50 m compared to Rögl et al. (1991) (Fig. 5a). Samples collected by Benda et al. (1979) (Gr 1401–1444) and two additional samples at the base of the Aghios Thomas section (Ag 1–2 in Fig. 5b), were analysed. Additionally, five outcrops of marine marls near Aegina city (AC 1–5) and scattered outcrops of marine marls and limestones in the northeast of the island near Aghia Marina (Fig. 1) were sampled (Gr 10.961–10.998) and analysed.

2. Biostratigraphy

Planktonic foraminiferal and calcareous nannoplankton biostratigraphies are based on the stratigraphical distribution of the early Pliocene marker species in the Mediterranean (Lourens et al., 2004, and references therein).

The samples collected for analysis of the foraminiferal content were washed and sieved with a 125 µm sieve; nannofossil samples were prepared according to standard preparation techniques (Bramlette and Sullivan, 1961).

2.1. Milos

Unit A contains only few fossil-bearing beds, without age-diagnostic biomarkers. Except for the

sandy base, Unit B in sections Akrotiraki and Tsouvala contains moderately to well-preserved foraminiferal and calcareous nannofossil assemblages.

The first occurrence (FO) of the planktonic foraminifer *Globorotalia puncticulata* is found both in the Akrotiraki-section (between Gr 10.473 and Gr 10.474) and in the Tsouvala-section (between Gr 10.160 and Gr 10.161; Fig. 4).

Three nannofossil bio-events are recorded: The FO of *Discoaster asymmetricus* between Gr 10.512 and Gr 10.513 in the Akrotiraki-section and between Gr 10.211 and Gr 10.212 in the Tsouvala-section; the FO of *Discoaster tamalis* between Gr 10.523 and 10.524 in the Akrotiraki section and between Gr 10.226 and Gr 10.227 in the Tsouvala-section (Fig. 4). The last common occurrence (LCO) of *Sphenolithus* spp. is recorded between Gr 10.524 and Gr 10.524a of the Akrotiraki section.

2.2. Aegina

Samples So 1–61 from the Souvala section (Unit 1 in Figs. 3b and 5a) did not contain any age-diagnostic nannofossils or foraminifera. In contrast, Rögl et al. (1991) reported the occurrence of *Ceratolithus acutus* from a single level in the section, a taxon belonging to the NN12 Zone sensu Martini (1971).

The two samples Ag 1–2 collected at the base of section Aghios Thomas (Unit 2 in Figs. 3b and 5b) are assigned to the upper part of the NN12 Zone, based on the absence of *Triquetrorhabdulus rugosus* and *C. rugosus* in combination with the co-occurrence of *Amaurolithus delicatus* and *Helicosphaera sellii*. Benda et al. (1979) reported the FO of *G. puncticulata* between Gr 1416 and 1417 and the FO of *D. asymmetricus* between Gr 1438 and 1439 (Fig. 5b). Two of the additionally collected samples from the northeast of Aegina (Gr 10.961–10.998) contained age-diagnostic nannofossil assemblages: Both Gr 10.983 and Gr. 10.997 (near Aghia Marina, Fig. 1) were assigned to NN13–14, based on the absence of *Pseudoemiliania lacunosa* and the abundance of *H. sellii*. Samples AC 4 and 5 belong to the NN14–15 Zone, based on the presence of *D. asymmetricus* and the absence of *D. tamalis*.

In summary, the biostratigraphy of the marine marls of Milos (Unit B) and Aegina (Unit 2) indicates that both units were deposited during the early Pliocene.

3. Magnetostratigraphy

The paleomagnetic samples were taken with a water-cooled, generator-powered electric drill and oriented with a magnetic compass. At least one specimen per sampling level was thermally demagnetised with small temperature increments of 20–50 °C up to a maximum temperature of 690 °C in a magnetically shielded, laboratory-built furnace. The natural remanent magnetisation (NRM) of the specimens was measured on a 2G Enterprises horizontal DC SQUID cryogenic magnetometer.

Almost all samples from sections Souvala, Akrotiraki and Kipos have very low intensities. In most cases, a normal polarity component is removed at temperatures between 100 and 210 °C. This relatively low-temperature component typically has a present-day field direction before bedding plane correction and can thus be regarded as a secondary, recent overprint, likely caused by weathering. After removal

of the low-temperature component, the remaining intensity of most samples of Akrotiraki and Kipos is too low to reliably interpret a characteristic remanent magnetisation (ChRM) direction from the demagnetisation diagrams (Fig. 6a; Zijdeveld, 1967), although occasionally a clear indication of the polarity of the ChRM can be interpreted (Fig. 6b). Some samples of the Souvala (Aegina), Akrotiraki and Kipos sections and most samples of the Tsouvala section show that a relatively high temperature component is gradually removed between temperatures of 210 and 390–450 °C or 580 °C (Fig. 6c and d). This component is taken as the ChRM.

Maximum unblocking temperatures in the range of 290–410 °C indicate that the NRM is (in part) carried by iron sulphides. In addition, magnetite is indicated as carrier of the magnetic signal considering the maximum unblocking temperature of ~ 580 °C. In some cases, a (normal polarity) high-temperature (up to 650 °C) haematite component is present in the

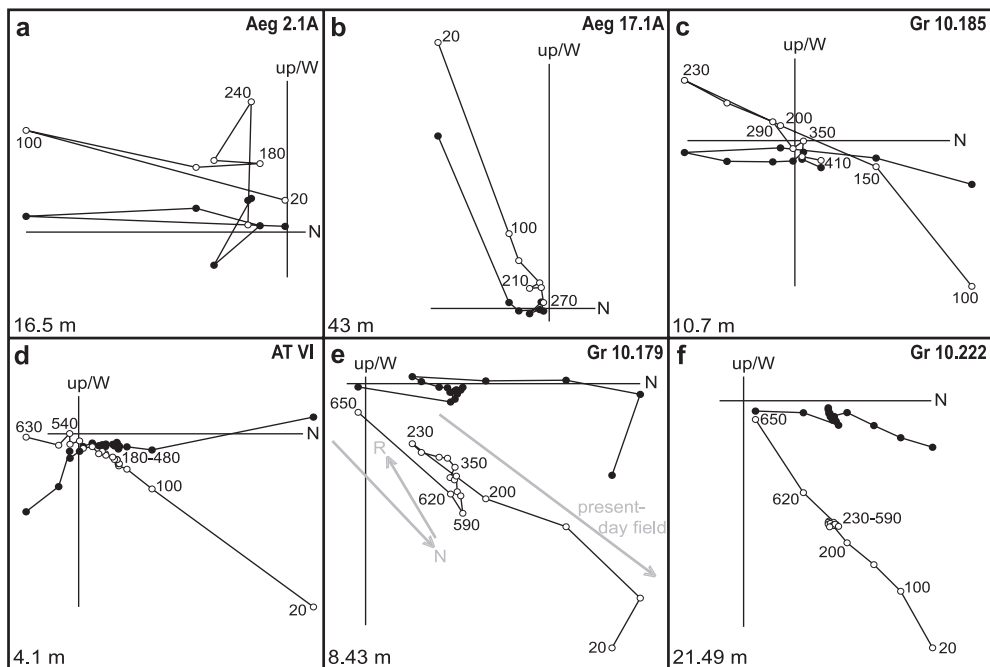


Fig. 6. Thermal demagnetisation diagrams of selected samples of the paleomagnetically analysed sections. Orthogonal projections with open (closed) symbols denote ChRM vector end-points (corrected for bedding tilt) on the vertical (horizontal) plane; values represent temperature increments in °C. Stratigraphic levels are in the lower left corners. (a) Inconclusive; (b) unreliable reversed; (c) reliable reversed (iron sulphide); (d) reliable normal (magnetite); (e) reliable reversed (magnetite) with normal maghaemite or haematite overprint and (f) inconclusive (either normal polarity with haematite as the carrier of the signal or reversed with magnetite as the carrier with an haematite overprint) ChRM directions.

Tsouvala-section, which is interpreted as a recent magnetisation (Fig. 6e). In some cases, these magnetite and haematite components have a largely overlapping unblocking temperature spectrum, resulting in a ‘cluster’ between 230 and 590 °C (Fig. 6f). In such cases no ChRM can be derived and these samples are represented by grey intervals in Figs. 4 and 5. Directions were calculated for each reliable ChRM component, after correction for bedding tilt.

In summary, the ChRM do not allow the construction of an unambiguous polarity zonation in section Akrotiraki (Fig. 4a). All samples of sections Kipos, Tsouvala and Souvala that can be reliably interpreted reveal a reversed polarity (Figs. 4 and 5a).

4. Age model

4.1. Age model for the Neogene deposits predating volcanism on Milos

Astronomical calibration of cyclic lithology alternations in late Miocene and Pliocene sections in the Mediterranean (e.g. Hilgen, 1991; Steenbrink et al., 1999; Lourens et al., 2004) has shown that these alternations can be tuned to the target curve of summer insolation of Laskar et al. (1993). This tuning has enabled the construction of astronomical polarity time scales (APTS).

The marine succession of Unit B on Milos reveals a cyclic pattern of marls and sapropels (Fig. 4a and b). Since the biostratigraphy indicates early Pliocene ages, a correlation to the Rossello composite section on Sicily (Langereis and Hilgen, 1991) can be attempted.

This correlation must mainly rely on the biostratigraphic events, since the magnetostratigraphy of our sections is insufficiently precise. The following bioevents recorded in the Tsouvala and Akrotiraki sections are correlated with those in the Rossello composite section (Lourens et al., 2004): the FO of *G. puncticulata* at 4.52 Ma (event A); the FO of *D. asymmetricus* at 4.12 Ma (event B); the FO of *D. tamalis* at 3.97 Ma (event C) and the LCO of *Sphenolithus* spp. at 3.70 Ma (event D; Fig. 7).

The framework provided by biostratigraphy can now be used for further astronomical tuning of the individual marl–sapropel cycles to the target-curve of Laskar et al. (1993) (Fig. 7). This tuning is based on

pattern correspondence between the marl–sapropel alternations and the cyclic variations in the intensity of summer insolation at 65°N caused by the interference of three Milankovitch cycles: the eccentricity (with a period of 400 and 100 kyr), obliquity (41 kyr) and precession (21 kyr). 400 kyr eccentricity minima result in ‘missing sapropels’, such as seen in cycles 40 and 41 (Fig. 7). In the 400 kyr eccentricity maxima, the interference between the 100 kyr eccentricity and precession cyclicity led to development of triplets (52–54) or quadruplets (48–51) of sapropels (Fig. 7). Finally, interference between obliquity and precession can be inferred from alternating clearly developed (32, 34) and poorly (35) or non-developed (33) sapropels (Fig. 7). Tuning of Tsouvala is rather straightforward, since the above-described patterns are clearly developed. Between 27 and 32 m in Akrotiraki, the patterns are less well developed and an apparent decrease in sedimentation rate occurred. The quadruplet of 48–51, however, is clear, as is the duplet 37–38. It follows that the age of the lowest sapropel in the Akrotiraki section (at 20.3 m, Fig. 7) is estimated at 5.0 Ma.

In the top 15 m of Unit B, sapropel–marl alternations are lacking, which impedes cyclostratigraphical correlation with the APTS. Moreover, the small stratigraphical distance (less than 1 m) between bioevents C and D in the upper part of the Akrotiraki section suggests the presence of a hiatus (-H- in Fig. 7). The age of the unconformably overlying volcanic series (3.5 ± 0.14 Ma and younger; Fytikas et al., 1986), however, provides the minimum age for the top of Unit B.

A reversed polarity is found for all reliable samples from the Tsouvala section. The correlation of the bioevents with the Rossello composite section indicates, however, that during the deposition of the Tsouvala-section at least three magnetic reversals must have occurred. This suggests that the reversed ChRM directions are caused by a post-depositional overprint during a reversed interval.

Although the magnetostratigraphic data obtained from the Akrotiraki section are of poor quality (Fig. 4a), the available results do not contradict the bio- and cyclostratigraphic correlations. This implies that the normal polarity of samples AT VI (4 m) and KP 2 (20 m) in the Akrotiraki section must be interpreted to belong to the Thvera subchron (C3n.4n: 5.236–4.998

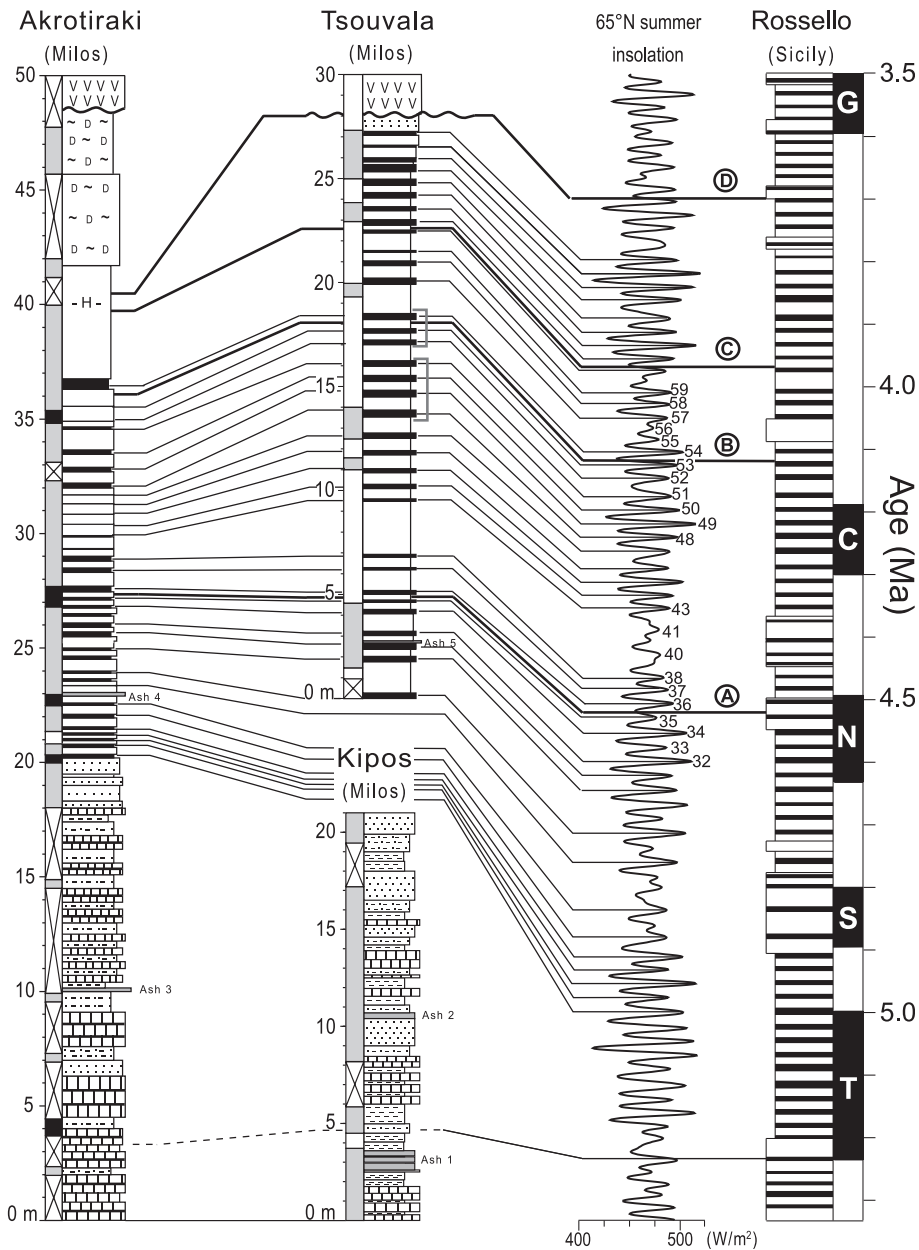


Fig. 7. Correlation of the sections of southern Milos to the 65°N summer insolation curve of Laskar (1993) and the cyclo- and magnetostratigraphy of the Rossello composite section (Lourens et al., 1996). Bio-events taken from Lourens et al. (2004). Thick solid tie lines are used to indicate bio-events: (A) FO *G. puncticulata* (4.52 Ma); (B) FO *D. asymmetricus* (4.12 Ma); (C) FO *D. tamalis* (3.97 Ma); (D) LCO *Sphenolithus* spp. (3.70 Ma). Dotted tie lines indicate magnetic reversals and thin solid lines represent the tuning of marl–sapropel alternations to the Laskar-curve. For lithology keys: see Fig. 3.

Ma: Lourens et al., 2004). The correlation of Unit A to the APTS is impossible, since no clear cycles can be distinguished.

From the 28 samples recovered from section Kipos, only samples Gr 10.560 and 10.561 (~ 4 m) give a conclusive ChRM direction, indicating a reversed

polarity. These levels are interpreted to correspond to the uppermost part of subchron C3r just below the Thvera subchron.

In summary, Unit A was deposited prior to ~ 5.0 Ma, the marine marls and sapropels of unit B have an age range of $\sim 5.0\text{--}3.5 \pm 0.14$ Ma, after which volcanism commenced.

4.2. Age model for the Neogene deposits predating volcanism on Aegina

The age of the basal conglomerates is estimated at 8–6 Ma by Rögl et al. (1991), based on the recovery of two teeth of an advanced species of *Hipparion* s.s. The nannofossil *C. acutus* at 45 m in the overlying Souvala section (Fig. 5a) has an age range of 5.372–5.046 Ma (Backman and Raffi, 1997). We thus interpret the reversed polarity between 21 and 48 m in the Souvala-section to belong to subchron C3r (6.04–5.236 Ma: Hilgen et al., 1995; Krijgsman et al., 1999), which is in good agreement with the ostracod and mollusc associations found between 25 and 50 m in the Souvala section (Fig. 5a), which have been assigned to the Pontian (Rögl et al., 1991; 6.15–5.3 Ma: Snel et al., in press).

The oldest open marine clays of the section of Aghios Thomas have a calcareous nannofossil assemblage that is characteristic for the upper part of the NN12 Zone, which ranges from 5.23 to 5.09 Ma (Backman and Raffi, 1997). The first occurrences of *G. puncticulata* and *D. asymmetricus* higher in the section (Benda et al., 1979; Fig. 5b) are calibrated to an age of 4.52 and 4.12 Ma, respectively (Lourens et al., 2004).

The marine marls in the northeast of the island near Aghia Marina (NN13–NN14; 5.09–4.0 Ma: Berggren et al., 1995a,b; Backman and Raffi, 1997) and the marls in the northwest near Aegina City (NN14–NN15; 4.12–3.97: Lourens et al., 2004) serve to illustrate, that marine sedimentation covered at least the entire northern part of Aegina during the early Pliocene (Fig. 1).

In summary, deposition of Unit 1 commenced before or at 8–6 Ma and lasted into at least the late Messinian. Unit 2 has early Pliocene ages, but the very base of the Pliocene has not been found. The age of the oldest lavas overlying Unit 2 is 3.87 ± 0.05 Ma (Müller et al., 1979; Pe-Piper et al., 1983), slightly older than those on Milos.

4.3. Age estimate of the oldest volcanic ash deposits on Milos

The oldest volcanic deposits that have been reported from Milos are the late early Pliocene lavas overlying Unit B (Fytikas, 1977; Fytikas et al., 1986). However, we found older volcanic ash layers within unit B that require some further discussion.

The biotite crystals in the volcanic ash layers in the Milos sections were too weathered to obtain reliable radiometric ages (K. Kuiper, pers. comm. 2001). Therefore, we estimate the ages of the ash layers by using the age model presented in paragraph 5.1 (Fig. 7).

The age estimate of Ash 1 (Fig. 7) is only based on the age of the overlying strata, which have a reversed polarity interpreted as subchron C3r, 6.04 to 5.236 Ma (Hilgen, 1991; Krijgsman et al., 1999). The possible age range of ashes 2 and 3 (Fig. 7) is determined by the normal polarity of the strata on top of and below Ash 3 in section Akrotiraki, interpreted as the Thvera subchron (C3n.4n: 5.236–4.998 Ma: Lourens et al., 2004). The age estimates of Ash 4 in Akrotiraki and of Ash 5 in Tsouvala (Fig. 4) are based on the correlation of the marl–sapropel cycles to the APTS (Fig. 7): 4.82 and 4.62 Ma, respectively. These volcanic ash layers and the one on Aegina with an age of 4.4 ± 0.2 Ma (Müller et al., 1979) may originate from the older volcanic centres of e.g. Antiparos or Patmos-Chiliomodi (Fig. 1), from which islands Fytikas et al. (1984) reported lavas with comparable ages. Thus, from the presented integrated stratigraphy can be concluded that a sequence of lower Pliocene marine sediments was deposited just prior to the onset of volcanism on Aegina and Milos indeed.

5. Paleobathymetry and vertical motions

Paleobathymetry analyses of the marine marls of Unit B on Milos and unit 2 on Aegina were carried out to explore any changes in bathymetry that occurred prior to the oldest volcanic activity. The paleobathymetry reconstructions are based on the general relation between the plankton fraction (%P) of the total foraminiferal population and depth (Van der Zwaan et al., 1990), following procedures for the reconstruction of vertical motions described by Van Hinsbergen et al. (submitted for publication).

The %*P* graphs versus time for both the Milos and Aegina sections are shown in Fig. 8A. The graphs of Milos include a moving average curve with the standard deviation calculated per moving interval; it was chosen in such a way, that approximately 100 kyr is averaged at every sample level. The obtained curves

give a similar trend, but the %*P* values derived for the Tsouvala section are slightly smaller than those of comparable ages obtained from the Akrotiraki-section.

The %*P* increase between ~5 and 4.4 Ma obtained from the Milos appears to take place in two distinct episodes. From the %*S* curves (percentage

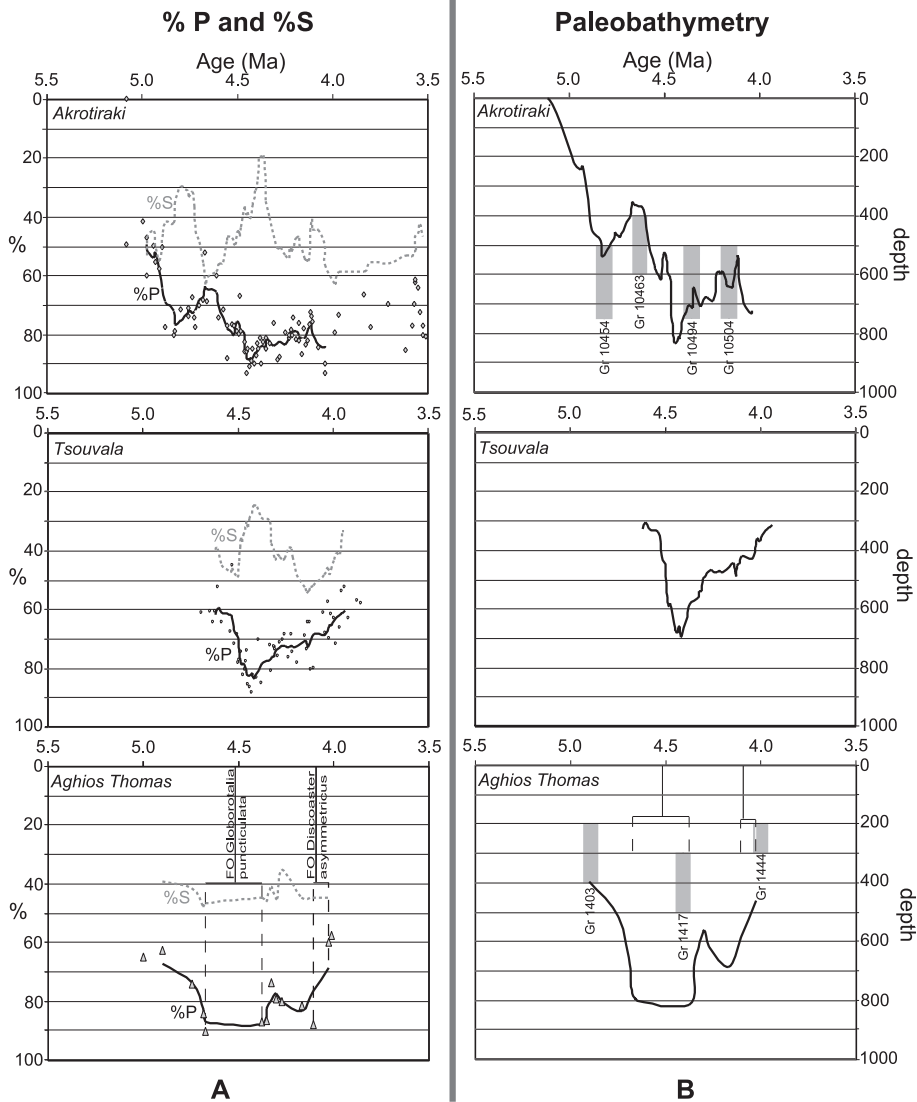


Fig. 8. (A,B) Paleobathymetry curves, determined from the Akrotiraki and Tsouvala sections on Milos and the Aghios Thomas section on Aegina, respectively. The moving averages are chosen to average approximately 100 kyr. The first occurrences (FO) of *G. puncticulata* and *D. asymmetricus* are included in the graphs for the Aghios Thomas section to indicate the uncertainty in the age determination of the Aghios Thomas samples. For the age determination of the Milos curves: see Fig. 7. B includes the bathymetry estimations based on the independent taxonomy check.

stress markers of the total number of benthic foraminifera) that are included in Fig. 8A, however, a strong cyclic oxygen-level variation can be concluded with a periodicity of 400 kyr. Generally, an oxygen level-driven %S increase results in a relative drop in %P, which, superimposed on a deepening trend, can explain the episode of %P-decrease in the curve of Fig. 8A (see Van Hinsbergen et al., submitted for publication, for further discussion on the relationship between %P, oxygen level and depth). The intervals of lowest %S are thus considered to represent actual depth and are connected to construct a depth-induced %P trend (Van Hinsbergen et al., submitted for publication).

The calculated paleobathymetry versus time graphs of the studied sections are shown in Fig. 8B. Following the scheme of Van Hinsbergen et al. (submitted for publication), an independent bathymetry check was carried out on selected samples of the Akrotiraki and Aghios Thomas sections, on the basis of selected benthic foraminifera, which are considered as depth markers. The results reveal benthic assemblages indicating biotope depth ranges that are in good agreement with the obtained depth values for the Akrotiraki section (Fig. 8B). The results for the Aghios Thomas section confirm the deepening trend, but may indicate that the calculated depth of 700–800 m is an over-estimation (Fig. 8B).

Now, paleobathymetry variations can be converted to (tectonically induced) vertical motions. For this purpose, three additional corrections were carried out: Firstly, the effects on paleobathymetry of sediment accumulation and compaction were corrected for. Furthermore, our high-resolution time-control makes it possible to accurately correct for the sea-level changes using the astronomically tuned sea-level curve of Lourens and Hilgen (1997).

Fig. 9 shows the thus obtained vertical motion curve constructed for the oldest Neogene of Milos and Aegina. The base of units A and 1 were taken as reference level. As a net result, during the deposition of units A and 1, sedimentation kept pace with subsidence and eustatic sea level changes.

The paleobathymetry record and age control, obtained from the Aghios Thomas section on Aegina are of much poorer resolution than those derived from the Milos sections, but they serve to illustrate that the non-marine to brackish-water sedimentation of the late Miocene was succeeded by the deposition of deep-marine early Pliocene sediments pre-dating the

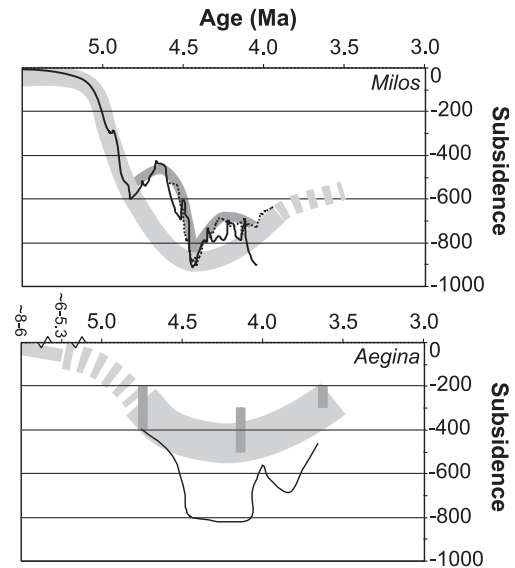


Fig. 9. Vertical motion curves for Milos and Aegina. The base of Units A and 1 were chosen as reference level for Milos and Aegina, respectively. Note that we follow the depth trend obtained from the qualitative depth markers on Aegina, which are considered to be more accurate than the calculated values, due to the high amount of stress-markers.

earliest volcanism. The trends in vertical motion on both islands are thus comparable and occur within the same time span.

6. Analysis

The debut of Neogene subsidence on Milos and Aegina is reflected by the onset of deposition of Unit A and Unit 1, respectively. On Aegina, the oldest datable deposits have an age range of 8–6 Ma (Rögl et al., 1991). Our suggestion that sedimentation generally kept pace with basin subsidence during the deposition of units A and 1 is supported by their respective lithologies, which are interpreted as representing alternating fluvial, brackish and shallow marine environments. Hence, approximately 80 m of subsidence during the deposition of units A and 1 is reconstructed (Fig. 9).

The ages derived from Unit 1 on Aegina indicate that upper Messinian (Pontian) strata are included in the stratigraphy. Unit A of Milos may also cover (part of) the Messinian, but conclusive evidence is lacking. During the late Messinian, the Messinian Salinity

Crisis occurred throughout the Mediterranean region (Krijgsman et al., 1999). However, both on Aegina and on Milos, no geologic evidence was found for the accompanying drastic sea level drop and subsequent rise. A dramatic relative sea level rise (~ 900 m) occurred around 5 Ma on Milos—i.e. approximately 300 kyr after the Pliocene Flooding, which ended the Messinian Salinity Crisis (Krijgsman et al., 1999). This relative sea level rise is interpreted as the consequence of tectonic subsidence. This is in line with the seismic profiles and submarine map tectonic maps of the Saronic Gulf of Papanikolaou et al. (1988), which shows a complex pattern of E–W, N–S and WNW–ESE trending normal faults, along which the WNW–ESE trending Saronic Gulf subsided in the Plio-Quaternary.

The comparable trends for Milos and Aegina shown in the curves of Fig. 9 suggests, that the high-resolution subsidence record obtained from Milos represents a regional rather than a local phenomenon. This is supported by a semi-quantitative paleobathymetry reconstruction carried out on DSDP core 378 in the Sea of Crete by Wright (1978) (Fig. 1), who estimated approximately 1000 m of early Pliocene deepening in the Cretan basin.

In summary, immediately prior to the onset of volcanism on the islands of Milos and Aegina, rapid subsidence occurred, with a maximum of approximately 1 km in the central Aegean. This subsidence is a regional phenomenon and is probably associated with large-scale extension in the southern and central Aegean.

We assume that the extension can be described by the stretching model of McKenzie (1978b). In this model, stretching-induced subsidence can be subdivided in an initial subsidence phase S_i , which is of

tectonic origin, followed by a thermal subsidence (or uplift) phase as a result of cooling of the welled up asthenosphere. Since the early Pliocene subsidence we determined from Milos and Aegina occurs rapidly, we consider this subsidence to correspond to S_i . The stretching factor β can be calculated from isostatic equilibrium conditions preceding and following the initial subsidence S_i . We simplified the model of McKenzie (1978b) by assuming constant densities for the crust ($\rho_c = 2850 \text{ kg/m}^3$), lithospheric mantle ($\rho_l = 3380 \text{ kg/m}^3$), sub-lithospheric mantle or asthenosphere ($\rho_m = 3300 \text{ kg/m}^3$) and seawater ($\rho_w = 1000 \text{ kg/m}^3$; Fig. 10):

$$\beta = (h_c \rho_c + (h_l - h_c) \rho_l - h_l \rho_m) / (h_c \rho_c + (h_l - h_c) \times \rho_l - h_l \rho_m - S_i \rho_w + S_i \rho_m) \quad (1)$$

where h_l is the initial thickness of the lithosphere including the crust and h_c is the initial thickness of the crust. Following McKenzie (1978b), we chose the initial thickness of the crust to correspond to the thickness of the present-day crust below mainland Greece, i.e. to approximately 40 km (Makris, 1977). We assume that the thickness of the lithosphere prior to extension h_l equals 100 km. Using Eq. (1), the rapid, 1 km subsidence we obtained from Milos yields a stretching factor β of ~ 1.2 .

McKenzie and Bickle (1988) determined that stretching of continental lithosphere generates only little melt, unless $\beta > 2$ and the (dry) mantle potential temperature exceeds 1380°C . Thus, it seems highly unlikely that the stretching associated with the rapid early Pliocene subsidence of Milos preceding volcanism led to melting of the underlying mantle.

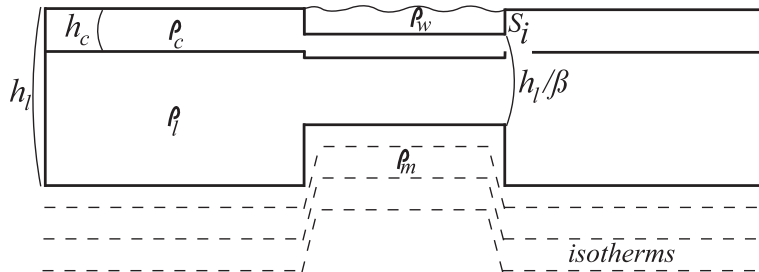


Fig. 10. Stretching model for the lithosphere simplified after McKenzie (1978b). See text for further explanation.

The magmas that were erupted in the Aegean during the early Pliocene probably must already have been present prior to the extension phase. The generation of the magmas is likely to have been caused by the addition of water to the mantle as a result of the subduction of the African plate, lowering the melting temperature, as was suggested based on geochemical data by Barton et al. (1983) and Briquieu et al. (1986).

Extension not only occurred on the site of the present-day volcanic centres but also e.g. in the Sea of Crete. The volcanic centres lie approximately at the 130–150 km isodepth line of a seismically defined north-dipping Benioff zone, interpreted to represent the top of the subducting African slab (Makropoulos and Burton, 1984; Hatzfeld, 1994; Giuchi et al., 1996; Papazachos et al., 2000). Hydrous minerals generally start to dehydrate when they are subducted to a depth of approximately 100–150 km (Philpotts, 1990). The position of the volcanic centres is thus probably determined by the depth of the subducted slab. The fact that during the early Pliocene rapid subsidence occurred prior to the onset of volcanism leads us to conclude that there is a causal relationship between extension and the timing of the onset of volcanism, probably by the generation of a network of extensional faults facilitating magma rise.

7. Summary and conclusions

To determine whether extension of the Aegean overriding lithosphere played a significant role in the formation and location of the early Pliocene volcanoes of the Aegean we aimed to reconstruct the a vertical motion history as it took place prior to the onset of volcanism. To this end we reconstructed the paleobathymetry evolution of selected sections in the lower Pliocene of Milos and Aegina using the general relationship between the percentage of planktonic foraminifera amongst the total population and depth. Age dating on the Milos sections was based on bio-magneto- and cyclostratigraphy; on Aegina only bio- and magnetostratigraphic dating was possible. About 900 m of subsidence occurred on Milos between ~ 5 and 4.4 Ma. Although less well constrained, a similar

history is reconstructed from Aegina. Volcanic eruptions followed 1–1.5 Ma after the onset of rapid subsidence. We used a simplified model, based on McKenzie (1978b), to show that adiabatic decompression is highly unlikely to have led to the generation of the melts that were erupted during the Pliocene on Milos and Aegina. The fact that the onset of volcanism is preceded by a regional phase of rapid subsidence, however, leads us to conclude that the timing of the formation of the volcanoes is probably the result of early Pliocene extension and the creation of associated faults, providing a way to the surface for pre-existing, subduction-related melts.

Acknowledgements

Francisco Sierro and David Piper are thanked for constructive reviews. Sampling of the Tsouvala section was carried out in 1997 by Frits Hilgen, Charon Duermeijer, Nicole van Vugt and Sandra Langezaal. Nicole van Vugt carried out the paleomagnetic analysis of these samples. Charon Duermeijer sampled and analysed the Souvala samples from Aegina. Constantin Doukas and Frosso Georgiades-Dikeoulia are thanked for their assistance in the Milos sampling campaign in 2000. Rob Lengkeek, Koenraad Elewaut, Maria Triantaphyllou and Yiannis Dimitriou are thanked for their assistance in sampling on Milos and Aegina in 2001. Frits Hilgen is acknowledged for his assistance in determining planktonic foraminifera. Bert van der Zwaan and Tanja Kouwenhoven are thanked for the fruitful discussions about the paleobathymetry-estimations and the determination of the benthic depth markers. Suzanne Bijl is acknowledged for the advice and discussion concerning the statistic analyses and Jason Herrin is thanked for discussion on volcanism and melt generation. Gerrit van 't Veld and Geert Ittman are thanked for the preparation of the samples used for foraminiferal analysis. This research was conducted under the research programs of the Vening Meinesz Research School of Geodynamics (VMSG) and the Netherlands Research school of Sedimentary Geology (NSG). This is a VMSG and NSG publication (NSG publication number 20030206).

References

- Backman, J., Raffi, I., 1997. Calibration of Miocene nannofossil events to orbitally tuned cyclostratigraphies from Ceara Rise. In: Shackleton, N.J., et al. (Eds.), *Proceedings of the Ocean Drilling Program Scientific Results*, 154, 83–99.
- Barton, M., Salters, V.J.M., Huijsmans, J.P.P., 1983. Sr isotope and trace element evidence for the role of continental crust in calc-alkaline volcanism on Santorini and Milos, Aegean Sea, Greece. *Earth Planet. Sci. Lett.* 63, 273–291.
- Benda, L., Jonkers, H.A., Meulenkamp, J.E., Steffens, P., 1979. Biostratigraphic correlations in the Eastern Mediterranean Neogene: 4. Marine microfossils, sporomorphs and radiometric data from the lower Pliocene of Ag. Thomas, Aegina, Greece. *Newsl. Stratigr.* 8, 61–69.
- Berggren, W.A., Hilgen, F.J., Langereis, C.G., Kent, D.V., Obradovich, J.D., Raffi, I., Raymo, M.E., Shackleton, N.J., 1995a. Late Neogene chronology: new perspectives in high-resolution stratigraphy. *GSA Bull.* 107, 1272–1287.
- Berggren, W.A., Kent, D.V., Swisher III, C.C., Aubry, M.-P., 1995b. A revised Cenozoic geochronology and chronostratigraphy, geochronology time-scales and global stratigraphic correlation. *SEPM Spec. Publ.* 54, 129–212.
- Bramlette, M.N., Sullivan, F.R., 1961. Coccolithophoreids and related nannoplankton of the early tertiary in California. *Micro-paleontology* 7, 129–188.
- Briqueu, L., Javoy, M., Lancelot, J.R., Tatsumoto, M., 1986. Isotope geochemistry of recent magmatism in the Aegean arc: Sr, Nd, Hf, and O isotopic ratios in the lavas of Milos and Santorini—geodynamic implications. *Earth Planet. Sci. Lett.* 80, 41–54.
- Fytikas, M., 1977. *Carte Géologique de Milos IGMR*, Athens.
- Fytikas, M., Innocenti, F., Manetti, P., Mazzuoli, R., Peccerillo, A., Villari, L., 1984. Tertiary to Quarternary evolution of volcanism in the Aegean region. In: Dixon, J.E. (Ed.), *The Geological Evolution of the Eastern Mediterranean*. *Geol. Soc. London Spec. Publ.* 17, 687–699.
- Fytikas, M., Innocenti, F., Kolios, N., Manetti, P., Mazzuoli, R., Poli, G., Rita, F., Villari, L., 1986. Volcanology and petrology of volcanic products of the island of Milos and neighbouring islets. *J. Volcanol. Geotherm. Res.* 28, 297–317.
- Gautier, P., Brun, J.-P., Moriceau, R., Sokoutis, D., Martinod, J., Jolivet, L., 1999. Timing, kinematics and cause of Aegean extension: a scenario based on a comparison with simple analogue experiments. *Tectonophysics* 315, 31–72.
- Giuchi, C., Kiratzi, A., Sabadini, R., Louvari, E., 1996. A numerical model of the Hellenic subduction zone: active stress field and sea-level changes. *Geophys. Res. Lett.* 23, 2485–2488.
- Hatzfeld, D., 1994. On the shape of the subducting slab beneath the Peloponnese, Greece. *Geophys. Res. Lett.* 21, 173–176.
- Hilgen, F.J., 1991. Extension of the astronomically calibrated (polarity) time scale to the Miocene/Pliocene boundary. *Earth Planet. Sci. Lett.* 107, 349–368.
- Hilgen, F.J., Krijgsman, W., Langereis, C.G., Lourens, L.J., Santarrelli, A., Zachariasse, W.J., 1995. Extending the astronomical (polarity) time scale into the Miocene. *Earth Planet. Sci. Lett.* 136, 495–510.
- Krijgsman, W., Hilgen, F.J., Raffi, I., Sierro, F.J., Wilson, D.S., 1999. Chronology, causes and progression of the Messinian salinity crisis. *Nature* 400, 625–655.
- Langereis, C.G., Hilgen, F.J., 1991. The Rossello composite: a Mediterranean and global reference section for the early to early late Pliocene. *Earth Planet. Sci. Lett.* 104, 211–225.
- Laskar, J., Joutel, F., Boudin, F., 1993. Orbital, precessional, and insolation quantities for the Earth from –20 Ma to +10 Ma. *Astron. Astrophys.* 70, 522–533.
- Le Pichon, X., Angelier, J., 1979. The Hellenic arc and trench system: a key to the neotectonic evolution of the Eastern Mediterranean area. *Tectonophysics* 60, 1–42.
- Lourens, L.J., Hilgen, F.J., 1997. Long-periodic variations in the earth's obliquity and their relationship to third-order eustatic cycles and late Neogene glaciations. *Quat. Int.* 40, 43–52.
- Lourens, L.J., Hilgen, F.J., Laskar, J., Shackleton, N.J., Wilson, D., 2004. The Neogene Period. In: Gradstein, F.M., Ogg, J.G., Smith, A.G. (Eds.), *A Geologic Time Scale 2004*. Cambridge Univ. Press, Cambridge (Chapter 20).
- Makris, J., 1977. Geophysical investigations of the Hellenides. *Hamb. Geophys. Einzelschr.* 34, 1–124.
- Makropoulos, K.C., Burton, P.W., 1984. Greek tectonics and seismicity. *Tectonophysics* 106, 275–304.
- Martini, E., 1971. Standard Tertiary and Quarternary calcareous nannoplankton zonation. In: Farinacci, A. (Ed.), *Proceedings II Planktonic Conference, Roma 1970*, vol. 2, pp. 739–785.
- McKenzie, D., 1978a. Active tectonics of the Alpine–Himalayan belt: the Aegean Sea and surrounding regions. *Geophys. J. R. Astron. Soc.* 55, 217–254.
- McKenzie, D., 1978b. Some remarks on the development of sedimentary basins. *Earth Planet. Sci. Lett.* 40, 25–32.
- McKenzie, D., Bickle, M.J., 1988. The volume and composition of melt generated by extension of the lithosphere. *J. Petrol.* 29, 625–679.
- Meulenkamp, J.E., 1979. The Aegean and the Messinian salinity crisis. *Proc. of the VI Coll. on the Geology of the Aegean Region*, vol. 3, pp. 1253–1263.
- Morris, A., 2000. Magnetic fabric and paleomagnetic analyses of the Plio-Quarternary calc-alkaline series of Aegina Island, South Aegean volcanic arc, Greece. *Earth Planet. Sci. Lett.* 176, 91–105.
- Müller, P., Kreuzer, H., Lenz, H., Harre, W., 1979. Radiometric dating of two extrusives from a Lower Pliocene marine section on Aegina Island, Greece. *Newsl. Stratigr.* 8, 70–78.
- Papanikolaou, D., Lykoussis, V., Chronis, G., Pavlakis, P., 1988. A comparative study of neotectonic basins across the Hellenic Arc: the Messiniakos, Argolikos and Southern Evoikos Gulfs. *Basin Res.* 1, 167–176.
- Papazachos, B.C., Karakostas, V.G., Papazachos, C.B., Scordilis, E.M., 2000. The geometry of the Wadati–Benioff zone and lithospheric kinematics in the Hellenic arc. *Tectonophysics* 319, 275–300.
- Pe, G.G., 1973. Petrology and geochemistry of volcanic rocks of Aegina, Greece. *Bull. Volcanol.* 37, 491–514.
- Pe, G.G., Piper, D.J.W., 1972. Volcanism at subduction zones; The Aegean area. *Bull. Geol. Soc. Greece* 9.
- Pe-Piper, G., Hatzipanagiotou, K., 1997. The Pliocene volcanic rocks of Crommyonia, western Greece and their implications for the early evolution of the South Aegean arc. *Geol. Mag.* 134, 55–66.

- Pe-Piper, G., Piper, D.J.W., 2002. The igneous rocks of Greece. The anatomy of an orogen: Berlin–Stuttgart. Gebrüder Borntraeger 573 pp.
- Pe-Piper, G., Piper, D.J.W., Reynolds, P.H., 1983. Paleomagnetic stratigraphy and radiometric dating of the Pliocene volcanic rocks of Aegina, Greece. *Bull. Volcanol.* 46, 1–7.
- Perissoratis, C., 1995. The Santorini volcanic complex and its relation to the stratigraphy and structure of the Aegean arc, Greece. *Mar. Geol.* 128, 37–58.
- Philpotts, A.R., 1990. Principles of Igneous and Metamorphic Petrology. Prentice Hall, Englewood Cliffs, NJ, 498 pp.
- Rögl, F., Bernor, R.L., Dermizakis, M.D., Müller, C., Stancheva, M., 1991. On the Pontian correlation in the Aegean (Aegina Island). *Newsl. Stratigr.* 24, 137–158.
- Snel, E., Marunteanu, M., Macalet, R., Meulenkamp, J.E., van Vugt, N., 2004. Late Miocene to Early Pliocene chronostratigraphic framework for the Dacic Basin, Romania. In: Agusti, J., Oms, O. (Eds.), Late Miocene to Early Pliocene Environments and Ecosystems in Eurasia. *Palaeogeogr. Palaeoclimatol. Palaeoecol.* (in prep.).
- Steckler, M.S., Watts, A.B., 1978. Subsidence of the Atlantic-type continental margin off New York. *Earth Planet. Sci. Lett.* 41, 1–13.
- Steenbrink, J., Van Vugt, N., Hilgen, F.J., Wijbrans, J.R., Meulenkamp, J.E., 1999. Sedimentary cycles and volcanic ash beds in the lower Pliocene lacustrine successions of Ptolemais (NW Greece): discrepancy between $^{40}\text{Ar}/^{39}\text{Ar}$ and astronomical ages. *Palaeogeogr. Palaeoclimat. Palaeoecol.* 152, 283–303.
- Van der Zwaan, G.J., Jorissen, F.J., De Stigter, H.C., 1990. The depth dependency of planktonic/benthonic foraminiferal ratios: constraints and applications. *Mar. Geol.* 95, 1–16.
- Van Hinsbergen, D.J.J., Kouwenhoven, T.J., Van der Zwaan, G.J., submitted for publication. Paleobathymetry in the backstripping procedure: distinguishing between tectonic and climatic effects on depth estimates. (In prep.).
- Watts, A.B., Karner, K.D., Steckler, M.S., 1982. Lithosphere flexure and the evolution of sedimentary basins. *Philos. Trans. R. Soc. London* 305, 249–281.
- Wright, R., 1978. Neogene paleobathymetry of the Mediterranean basin on benthic foraminifers from DSDP leg 42A. In: Hsü, L., Montadert, L., et al. (Eds.), Initial Reports of the Deep Sea Drilling Project XLII, pp. 837–846.
- Zijderveld, J.D.A., 1967. A.c. demagnetisation of rocks: analysis of results. In: Collinson, D.W. et al., (Ed.), *Methods in Palaeomagnetism*. Elsevier, Amsterdam, pp. 254–286.